ELSEVIER

Biochimica et Biophysica Acta 1321 (1997) 195–199

BIOCHIMICA ET BIOPHYSICA ACTA
BBA

Rapid report

# Direct observation of spectral substructure in the $Q_y$-absorption band of light harvesting complex II by nonlinear polarisation spectroscopy in the frequency domain at low temperature

Axel Schubert [a], Bernd Voigt [b], Dieter Leupold [b], Wichard Beenken [b], Jürgen Ehlert [b], Paul Hoffmann [a], Heiko Lokstein [a,*]

[a] *Institut für Biologie, Humboldt-Universität zu Berlin, Unter den Linden 6, D-10099 Berlin Germany*
[b] *Max-Born-Institut für Nichtlineare Optik und Kurzzeitspektroskopie, Rudower Chaussee 6, D-12489 Berlin, Germany*

Received 13 May 1997; revised 23 June 1997; accepted 25 June 1997

**Abstract**

The unique high spectral resolution resulting from application of nonlinear polarisation spectroscopy in the frequency domain at 77 K directly reveals 6 subbands (at 649, 657, 667, 672, 675 and 679 nm) in the chlorophyll *a / b* $Q_y$-region of trimeric light-harvesting complex II. A shortening (from about 90 to 35 fs) of the corresponding dephasing times towards the 'blue' edge of the $Q_y$-band was observed. © 1997 Elsevier Science B.V.

*Keywords:* Chlorophyll form; Dephasing; Energy transfer; Nonlinear laser spectroscopy; Photosynthetic antenna complex

Light capture and efficient excitation energy transfer (EET) to the photosynthetic reaction centers is assured in higher plants by chlorophyll (Chl) *a* and *b* containing light-harvesting complexes (LHCs) [1]. Most abundant is LHC II, the mainly photosystem II associated antenna. The structure of LHC II is known to 3.4 Å resolution revealing the association of at least 12 Chls [2]. The current resolution, however, allows neither to distinguish between Chls *a* and *b* nor satisfactory interpretation of optical spectra in terms of the structural model. In particular, the considerable broadening of the $Q_y$-absorption region is a matter of debate. The broadening is generally attributed to spectral heterogeneity, i.e. the existence of shifted (when compared to monomeric Chl in solution) and overlapping transitions, so called Chl-forms [3]. Twelve such forms have been supposed for trimeric LHC II [4]. However, there is no consensus on their number, transition energies and function, yet. Neither is known whether they originate from excitonic interactions among Chls, coupling to the protein matrix or a combination of both. Thus the prevailing mechanism of the observed ultrafast EET between the Chl-forms is still discussed [5]. Distances of 9 to 14 Å as revealed by electron crystallography [2] and circular dichroism spectra [4,6] indicate excitonic interactions between neighbouring Chls. Thus coherent EET could be possible as well as Förster-type 'hopping' [5]. To distinguish between both mechanisms

Abbreviations: Chl, chlorophyll; EET, excitation energy transfer; LHC II, light-harvesting complex II; NLPF, nonlinear polarisation spectroscopy in the frequency domain

* Corresponding author: Tel.: +49 30 20936477; fax: +49 30 20936337; e-mail: heiko = lokstein@rz.hu-berlin.de


*PII* S0005-2728(97)00061-3

the ratio of dephasing time ($T_2$) and EET time is meaningful [5,7].

During the past decade several time and frequency domain techniques were employed to investigate these ultrafast processes [8–12]. A novel approach was introduced by us using nonlinear polarisation spectroscopy in the frequency domain (NLPF) [13,14] – a pump-probe laser spectroscopic technique based on a four-wave mixing process. The NLPF technique was described originally by Song et al. [13]. Thus the principle of NLPF is only briefly accounted for in Fig. 1. NLPF has several advantages when used to study heterogeneously broadened systems [15,16]. The $\chi^{(3)}$-dependence of the NLPF line-shape function provides better separation of substructures as compared to absorption experiments. As a frequency domain technique NLPF allows selective excitation of individual electronic transitions when compared to fs time-domain experiments. NLPF spectra directly indicate the spectral broadening mode(s). Dephasing times on the ps to fs scale can be obtained. NLPF facilitates investigations from (physiologically relevant) room temperature down to cryogenic temperatures. The NLPF technique was recently applied to study photosynthetic antennna complexes of higher plants as well as of purple bacteria at room temperature [17–19]. Here the first NLPF experiments at low temperature (77 K) are reported.

LHC II was prepared from fresh pea leaves (*Pisum sativum* L.) according to the procedure of Krupa et al. [20]. Trimeric LHC II samples were obtained at 110 mg ml$^{-1}$ Chl $a+b$ suspended in a buffered (10 mM Tricine, pH 7.8) solution of 67% glycerol and 1% n-octyl ß-D-glucopyranoside. The samples were cooled down to 77 K in a cuvette selected for low birefringence using a dynamic cryostate (Oxford). Samples keep optically clear at low temperature, but cooling may lead to depolarisation due to tension birefringence. Thus usually only a small volume of the sample can be used for NLPF measurements.

The experimental set-up has been described in detail previously [19]. Both, pump and probe beams were obtained from dye lasers being pumped simultaneously by an excimer laser. DCM dissolved in DMSO was used as laser dye. Both pulses had a spectral width of less than 0.05 cm$^{-1}$ and a duration of about 15 ns (FWHM). NLPF spectra were obtained by tuning the pump laser beam from 645 to 685 nm with the probe laser wavelength fixed at 675 nm. Pump beam intensities of $2 \cdot 10^{23}$ photons s$^{-1}$ cm$^{-2}$ were used; the probe beam intensity was about 100 times smaller. The validity of the $\chi^{(3)}$-approach for interpretation of the spectra was assured by the observed quadratic dependence of the NLPF signal on pump beam intensity [13].

A NLPF spectrum of trimeric LHC II measured at 77 K is compared to the absorption profile at the same temperature in Fig. 2. Significant substructure is obvious in the NLPF profile. Even at the first glance five peaks (at 649, 657, 667, 675 and 679 nm)

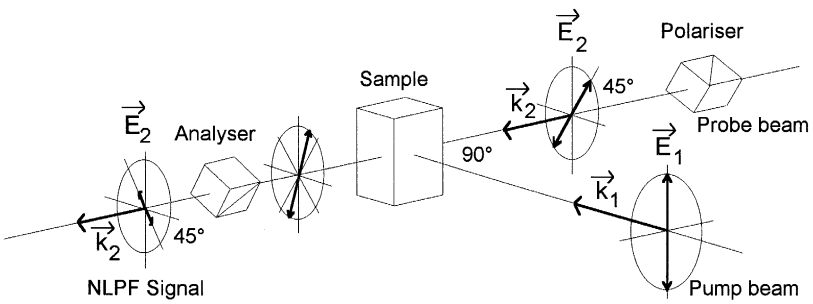


Fig. 1. Principle of nonlinear polarisation spectroscopy in the frequency domain (NLPF). The sample is located between two crossed polarisers. Pump and probe field (with $\vec{k}_{1,2}$ and $\vec{E}_{1,2}$ denoting the wave vectors and electrical field vectors, respectively) are highly monochromatic and linearly polarised at an angle of 45°. NLPF spectra are obtained by measuring polarisation changes of the weak probe field with fixed frequency $\omega_2(\omega = 2\pi c/\lambda)$ passing an absorbing medium in the presence of a strong pump field with the tuned frequency $\omega_1$. The NLPF signal is detected behind the analyser in the direction and at the frequency of the probe field. The signal represents the response of the probe field on a pump-field induced anisotropy in the sample, leading to dichroism. In theoretical terms the NLPF signal can be described as the degenerated $\chi^{(3)}$-response of the sample (lower orders are not contributing). Measurements are performed under stationary conditions, i.e. the duration of the laser pulses is considerably longer than the longest relaxation time in the system under investigation.

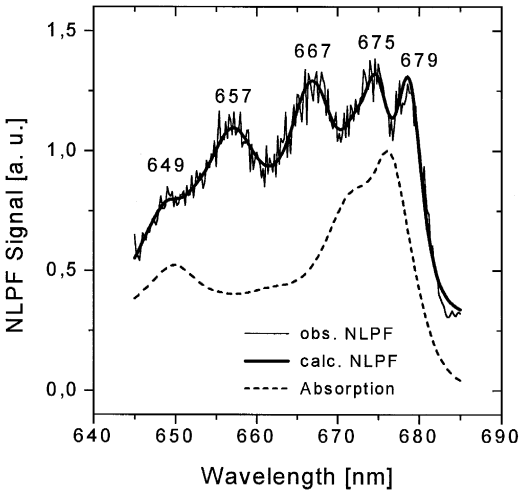


Fig. 2. Comparison of the NLPF spectrum (obtained at a probe wavelength of 675 nm) and the $Q_y$-absorption spectrum of trimeric LHC II at 77 K. Numbers indicate the transition wavelengths of the resolved spectral forms.

can be distinguished. (A shoulder at around 672 nm indicates a further transition, vide infra.) These Chl-forms have been deduced previously from indirect techniques [4,21] and are here revealed directly for the first time. Additionally, the well-resolved spectrum allows to deduce $T_2$ with high accuracy by curve-fitting. In our previous work the NLPF spectra of LHC II obtained at room temperature were fitted using a model consisting of several homogeneously broadened transitions without coupling among them [18]. Each transition was assumed to belong to a separate two level system, resulting in the following line shape function ($s$):

$$s(\omega_{01}) = \frac{i\alpha}{\Gamma + i\omega_{02}}\left[\frac{1}{\gamma}\left(\frac{1}{\Gamma + i\omega_{01}} + \text{c.c.}\right) + \frac{1}{\gamma + i\Delta}\left(\frac{1}{\Gamma + i\omega_{02}} + \frac{1}{\Gamma - i\omega_{01}}\right)\right] \quad (1)$$

with $\Gamma = T_2^{-1}$, $\gamma = T_1^{-1}$, $T_1$: energy relaxation time, $\Delta$: detuning of pump and probe frequency, $\omega_{01}$: detuning between pump frequency and the transition frequency, $\omega_{02}$: difference between probe frequency and the transition frequency, $\alpha$: scaling parameter. The total NLPF spectrum is obtained by the square module of the sum over the line shape functions of all transitions. In the line shape function (Eq. (1)) the first summand

$$\frac{1}{\Gamma + i\omega_{01}} + \text{c.c.} \quad (2)$$

describes the broad band part of the spectrum. The width of this band, representing the homogeneous linewidth of the transition, is determined by $T_2$ and *not dependent* on the model used. Only the prefactor of the summand may vary, leading to different absolute contributions of individual subbands to the NLPF spectrum in comparison to the absorption profile. The other summand contributes only to a narrow peak around the probe frequency, which vanishes in a broad band spectrum [16]. Thus this spectrum can be fitted properly using only the first summand (Eq. (2)) in the line shape function and varying the bandwidths, transition frequencies and the prefactors. The resulting (fitted) spectrum is also displayed in Fig. 2. $T_2$ and $\lambda_0$ as obtained by the best fit are presented in Table 1. A satisfactory fit was only possible including an additional band centered at 672 nm. From the data in Table 1 it is obvious that $T_2$ is shortened towards the 'blue' edge of the spectrum, as already visible in broadened bandwidths of the resolved subbands (Fig. 2). This phenomenon deduced from earlier NLPF measurements at room temperature [18], is now confirmed. Since $T_2$ is dependent on the energy relaxation time ($T_1$) as well as on the pure dephasing time ($T_2^*$),

$$\frac{1}{T_2} = \frac{1}{2T_1} + \frac{1}{T_2^*} \quad (3)$$

$T_2$-shortening can be explained in two ways: (i) It is caused by shorter $T_1$ due to fast EET away from

Table 1
Parameters obtained from fitting of the 77 K-NLPF spectrum as displayed in Fig. 2 ($\lambda_0$ indicates the transition wavelength of the subband; $T_2$ is the phase relaxation time)

| $\lambda_0$ (nm) | 648.6 | 657.0 | 666.8 | 672.4 | 674.8 | 678.9 |
|---|---|---|---|---|---|---|
| $T_2$ (fs) | 34 | 45 | 43 | 90 | 80 | 87 |

Errors of the transition wavelength determinations are about 1 nm; $T_2$ values were obtained with an accuracy of about 5%, assuming pure homogeneous broadening.

'blue'-shifted spectral forms. Assuming that no energy transfer occurs from the red-most shifted form (at 679 nm) results in a $T_2^*$ of about 90 fs for this subband. If, furthermore, this value for $T_2^*$ is assumed to be common for all subbands, EET times of less than 50 fs can be deduced following Eq. (3) for the Chl-forms centered at 649, 657 and 667 nm. This seems to be extremely fast, but on the other hand recent fs time-domain studies indicate EET times shorter than 300 fs [12] or even 150 fs [22] for the form at approximately 649 nm. (ii) Supposed that at 77 K for *all* Chl-forms $T_2 \approx T_2^*$, stronger vibronic coupling to the protein matrix has to be assumed for the blue-shifted forms. A contribution of both effects to the observed dephasing rates is also possible.

Comparison of NLPF spectra obtained at room temperature and at 77 K reveals considerably different spectral profiles (Fig. 3). One subband (centered at 684 nm) clearly contributing to the room temperature spectra is virtually absent in both, NLPF and absorption spectra at 77 K. Since this subband has been assigned to a transition from the first vibronic excited state [21] such behaviour has to be expected. The unique subband resolution (as compared to absorption spectra) and the marked contributions of short wavelength bands in the 77 K NLPF spectra, however, can not be explained by the previously used model of uncoupled two level systems (cf. [18]). For LHC II excitonic coupling among Chls has to be assumed (vide supra), but a comprehensive NLPF theory including it has not been available until now. However, preliminary theoretical considerations suggest that all transitions coupled to the spectral form selected by the probe field can show an enhanced contribution to the NLPF spectrum, presuming that coherence of the excitonic wave function is not destroyed by fast dephasing. $T_2^*$ is considerably longer at 77 K than at room temperature, since vibronic coupling to the environment is less pronounced. Hence, one can hypothesise that the displayed NLPF spectrum at 77 K features mainly transitions that are excitonically coupled to the 675 nm band.

The presented picture of the spectral substructure in the Chl *a*/*b*-$Q_y$-region of LHC II is hardly accessible with other techniques. Additionally, the spectrum reveals an extended, intricate excitonic coupling between spectral forms. Finally, the technical feasibility of NLPF investigations at low temperature has been demonstrated. Further extension to even lower temperatures appears to be generally desirable thus facilitating direct comparison to results obtained with other techniques, in particular nonphotochemical hole burning spectroscopy [11].

This work was supported by the Deutsche Forschungsgemeinschaft (grants Ho 1757/2-1 and Le 729/2-2). We are grateful to Mr. T. Schrötter (Institut für Physik, Humboldt-Universität zu Berlin) for fruitful discussions and measuring the 77 K absorption spectrum of LHC II.

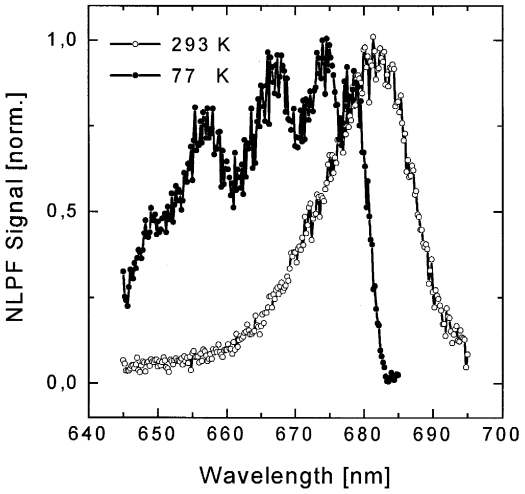


Fig. 3. Comparison of NLPF spectra of trimeric LHC II obtained at 77 and 293 K (probe wavelength 675 nm).

## References

[1] S. Jansson, Biochim. Biophys. Acta 1184 (1994) 1–19.
[2] W. Kühlbrandt, D.N. Wang, Y. Fujiyoshi, Nature 367 (1994) 614–621.
[3] J.S. Brown, Annu. Rev. Plant. Physiol. 23 (1972) 73–86.
[4] S. Nussberger, J.P. Dekker, W. Kühlbrandt, B.M. van Bolhuis, R. van Grondelle, H. van Amerongen, Biochemistry 33 (1994) 4775–14783.
[5] R. Van Grondelle, J.P. Dekker, T. Gillbro, V. Sundström, Biochim. Biophys. Acta 1187 (1994) 1–65.
[6] P.W. Hemelrijk, S.L.S. Kwa, R. van Grondelle, J.P. Dekker, Biochim. Biophys. Acta 1098 (1992) 159–166.
[7] J.A. Leegwater, J. Phys. Chem. 100 (1996) 14403–14409.
[8] D. Leupold, H. Stiel, E. Klose, P. Hoffmann, Ber. Bunsenges. Phys. Chem. 93 (1989) 371–374.
[9] D.D. Eads, E.W. Castner, R.S. Alberte, L. Mets, G.R. Fleming, J. Phys. Chem. 93 (1989) 8271–8275.

[10] M. Du, X. Xie, L. Mets, G.R. Fleming, J. Phys. Chem. 98 (1994) 4736–4741.
[11] N.R.S. Reddy, H. van Amerongen, S.L.S. Kwa, R. van Grondelle, G.J. Small, J. Phys. Chem. 98 (1994) 4729–4735.
[12] H.M. Visser, F.J. Kleima, I.H.M. van Stokkum, R. van Grondelle, H. van Amerongen, Chem. Phys. 210 (1996) 297–312.
[13] J.J. Song, J.H. Lee, M.D. Levenson, Phys. Rev. A 17 (1978) 1439–1447.
[14] S. Saikan, J. Sei, J. Phys. Chem. 79 (1983) 4146–4153.
[15] A.O. Marcano, L. Marquez, L. Aranguren, M. Salazar, J. Opt. Soc. Am. B. 11 (1990) 2145–2149.
[16] E. Neef, S. Mory, Exp. Techn. Phys. 39 (1991) 385–388.
[17] F. Nowak, B. Voigt, D. Leupold, M. Bandilla, H. Scheer, R.J. Cogdell, In: P. Mathis (Ed.), Photosynthesis: From Light to Biosphere, Kluwer, Dordrecht, 1995, vol. 1, pp. 151–154.
[18] H. Lokstein, D. Leupold, B. Voigt, F. Nowak, J. Ehlert, P. Hoffmann, G. Garab, Biophys. J. 69 (1995) 1536–1543.
[19] H. Lokstein, D. Leupold, B. Voigt, F. Nowak, J. Ehlert, P. Hoffmann, In: P. Mathis (Ed.), Photosynthesis: From Light to Biosphere, Kluwer, Dordrecht, 1995, vol. 1, pp. 287–290..
[20] Z. Krupa, N.P.A. Huner, J.P. Williams, E. Maissan, D.R. James, Plant Physiol. 84 (1987) 19–24.
[21] G. Zucchelli, F.M. Garlaschi, R.C. Jennings, Biochemistry 35 (1996) 16247–16254.
[22] T. Bittner, K.-D. Irrgang, G. Renger, M.R. Wasielewski, J. Phys. Chem. 98 (1994) 11821–11826.